理學博士學位論文

Mechanisms of pH regulation in rat trigeminal ganglion neurons

삼차신경절 신경세포의 pH 조절기전

2013 년 12 월

서울대학교 대학원
치의과학과 신경생물학 전공
황 성 민

Mechanisms of pH regulation in rat trigeminal ganglion neurons

by

Sung-Min Hwang

Advisor:

Prof. Kyungpyo Park, D.D.S., Ph.D.

December, 2013

Department of Neurobiology in School of Dentistry, Seoul National University

Abstract

The effect of intracellular acidification and subsequent pH recovery in sensory neurons has not been well characterized. I have studied the mechanisms underlying Ca^{2+}-induced acidification and subsequent recovery of intracellular pH (pH_i) in rat trigeminal ganglion (TG) neurons and report their effects on neuronal excitability. Glutamate (500 μM) and capsaicin (1 μM) increased intracellular Ca^{2+} concentration ($[Ca^{2+}]_i$) with a following decrease in pH_i. The recovery of $[Ca^{2+}]_i$ to the pre-stimulus level was inhibited by $LaCl_3$ (1 mM) and O-vanadate (10 mM), a plasma membrane Ca^{2+}/ATPase (PMCA) inhibitor. Removal of extracellular Ca^{2+} also completely inhibited the acidification induced by capsaicin. TRPV1 was expressed only in small and medium sized TG neurons. mRNA for Na^+/H^+ exchanger type 1 (NHE1), pancreatic Na^+-HCO_3^- cotransporter type 1 (pNBC1), NBC3, NBC4 and PMCA types 1-3 were detected by RT-PCR. pH_i recovery was significantly inhibited by pretreatment with NHE1 or pNBC1 siRNA. I found that the frequency of action potentials (AP) was dependent on pH_i. Application of the NHE1 inhibitor 5'-(N-ethyl-N-isopropyl) amiloride (5 μM; EIPA) or the pNBC1 inhibitor 4',4'-di-isothiocyano-stilbene-2',2'-sulfonic acid (500 μM; DIDS) delayed pH_i recovery and decreased AP frequency. Simultaneous application of EIPA and DIDS almost completely inhibited APs.

In summary, These results demonstrate that the rise in $[Ca^{2+}]_i$ in sensory neurons by glutamate and capsaicin causes intracellular acidification by activation of PMCA type 3, that the pH_i recovery from acidification is mediated by membrane transporters NHE1 and pNBC1 specifically, and that the activity of these transporters has direct consequences for neuronal excitability.

Key words: Trigeminal ganglion, Intracellular pH, Action potentials, Transient receptor potential vanilloid 1, Plasma membrane Ca^{2+}/ATPase, Na^{+}/H^{+} exchangers, Na^{+}/HCO_3^{-} cotransporters

Student number: 2004-30761

Contents

List of Figures

Abbreviations

AP	Action potential
BCECF	2',7'-bis-(2-carboxyethyl)-5',6'-arboxyfluorescein
BBS	Bicarbonate buffered solution
($[Ca^{2+}]_i$)	Cytoplasmic free Ca^{2+} concentration
DIDS	4',4'-diisothiocyanostilbene-2',2'-sulfonic acid
EIPA	5'-(N-Ethyl-N-isopropyl) amiloride
HSG	Human submandibular duct cell line
HBS	HEPES-buffered solutions
NHE	Na^+/H^+ exchanger
NBC	Na^+/HCO_3^- cotransporter
NDCBE	Na^+-dependent Cl^-/HCO_3^- exchanger
PMCA	Plasma membrane Ca^{2+}/ATPase
RT	Reverse trnascription
TRPV1	Transient receptor potential vanilloid1
TG	Trigeminal ganglion

This work has been reproduced from an article published by Sung-Min Hwang, Na-Youn Koo, Meihong Jin, Alexander J. Davies, Gae-Sig Chun, Se-Young Choi, Joong-Soo Kim and Kyungpyo Park. 2011. JBC, 286:1719-1729.

1. Introduction

Trigeminal ganglion (TG) neurons are primary sensory neurons that innervate deep and superficial tissues of the head and face [1]. They contain cell bodies of incoming sensory fibers [2]. The three major branches of the trigeminal nerve, ophthalmic nerve, maxillary nerve, and mandibular nerve converge on the trigeminal ganglion [1]. Also, trigeminal nerves are responsible for sensations of touch on the side of face, and have motor nerve fibers for motion [3]. The trigeminal ganglion functions as a link between external stimulation of the trigeminal nerve and the central nervous system [1]. The sensory fibers of the trigeminal nerves pass to the trigeminal ganglion, which in turn pass the nerve impulse through a single large sensory root that enters the brain stem to provide tactile and nociceptive afference of the face and mouth. TG neurons express a variety of neurotransmitter receptors [4]. Receptor activation changes the concentration of various ions in the cytoplasm, which in turn may affect neuronal excitability [5].

Various physiological and pathophysiological conditions can induce a change in the intracellular pH (pH_i). Many biological processes such as enzyme activity, ionic conductance and activity of membrane transporters are pH sensitive [6,7]. Thus, the regulation of pH_i in neurons is of critical importance; failure to maintain pH_i may lead to numerous pathophysiological conditions [8,9]. Neurons can be acidified in response to neurotransmitters and chemical compounds [10,11,12] and this intracellular acidification has been linked to the activity of the plasma membrane Ca^{2+}/ATPase (PMCA) [13,14]. For example, the PMCA was implicated in neurotransmitter-induced intracellular acidification in cerebellar granule cells [11,15], aortic vascular smooth muscle

cells [13] and pancreatic acinar cells in the rat [16,17]. In addition to the PMCA, it has been reported that Na^+/Ca^{2+} exchange and mitochondrial Ca^{2+} uptake also affect pH_i [5]. However, the underlying mechanisms for acidification and subsequent pH_i recovery in sensory neurons remain largely unknown.

Glutamate, the most ubiquitous excitatory neurotransmitter, increases cytoplasmic free Ca^{2+} ($[Ca^{2+}]_i$) in neurons delivering transmission of sensory information [10,11,12]. Also, capsaicin, the primary pungent compound in hot pepper, evokes changes in $[Ca^{2+}]_i$ in sensory neurons by activation of the transient receptor potential vanilloid 1 receptor (TRPV1)[18,19,20]. These compounds, as well as other neurotransmitters and chemicals, have been shown to evoke intracellular acidification through an increase in $[Ca^{2+}]_i$ in sensory neurons [5,21]. Thus, it is important for these cells to maintain physiological pH_i under conditions that otherwise may induce cell acidification. In addition, intracellular alkalization is known to activate nociceptors through activation of TRPA1 [7]. TRPV1 also is activated by both extracellular acidification and intracellular alkalization in dorsal root ganglion (DRG) neurons [6]. The acidification induced by either neurotransmitters or other receptor agonists is likely reversed by membrane transporters such as Na^+/H^+ exchangers (NHEs), Na^+/HCO_3^- cotransporters (NBCs) and Na^+-dependent Cl^-/HCO_3^- exchangers (NDCBEs)[14,22,23,24,25].

To date, the mechanisms of intracellular acidification have not been well characterized and the membrane transporters involved in pH_i recovery in primary sensory neurons, including trigeminal ganglion (TG), have yet to be identified. Therefore, the purpose of this study was to investigate the mechanism of intracellular acidification elicited by the glutamate and capsaicin-induced $[Ca^{2+}]_i$ increase in TG neurons. I have identified the pH_i regulatory

mechanisms induced by intracellular acidification and also show that inhibition of NHE subtype 1 (NHE1) and pancreatic NBC subtype 1 (pNBC1) specifically, leads to intracellular acidification and results in altered excitability of TG neurons.

2. Materials and Methods

Cell preparation

Procedures were carried out in accordance with the Institutional Animal Care and Use Committee (IACUC) at the School of Dentistry, Seoul National University. Briefly, neonatal Sprague-Dawley rats were anesthetized by ether and decapitated. Bilateral trigeminal ganglia were dissected and rinsed with Hanks' Balanced Salt Solution (HBSS) buffer (Gibco). In fresh HBSS buffer, each ganglion was cut into 10-15 tissue pieces and incubated at 37ºC in a 15-ml conical tube containing 3 ml of trypsin solution (final conc. 0.2%)(Gibco) for 30 min; the trypsin was removed and washed with warmed Dulbecco's Modified Eagle Medium (DMEM) (Sigma). Ganglia were triturated with a glass pasteur pipette in 2 ml fresh DMEM. Turbid media was removed to a second conical tube and the process was repeated twice more. With a final volume of 5 ml, the cell suspension was centrifuged at 550 *g* for 5 min, and the supernatant was discarded. The final suspension volume was varied according to the desired plating density: cell pellets were re-suspended in 0.5~1 ml DMEM media and applied as a single drop (approximately 200 μl) at the center of five to eight coverslips placed within 35-mm tissue culture dishes. Glass coverslips had been soaked in ethanol (100%, v/v) for 30 min and dried. The coverslips were then coated with poly-l ornithine (BD biosciences) and subsequently washed 3 times in distilled water [26]. To allow cell adhesion, cells were incubated (37ºC, 5% CO_2) for at least 1 hr before feeding. Cells were fed with 2 ml fresh DMEM and plates were incubated again for 1 hr (37ºC, 5% CO_2).

Measurement of $[Ca^{2+}]_i$ and pH_i

Cultured TG neurons were loaded with 2 μM 2',7'-Bis-(2-carboxyethyl)-5,6-arboxyfluorescein acetoxymethyl ester (BCECF-AM)(Molecular Probes, Eugene, OR) by directly adding stock solution to the culture medium followed by incubation for 30 min. BCECF-AM was prepared from a stock solution in DMSO; the final concentration of DMSO during loading was 0.1%. Fura-2-AM (Molecular Probes, Eugene, OR) was used to determine $[Ca^{2+}]_{i.}$. Cultured TG neurons were loaded by the addition of 2 ml of 2 μM Fura-2-AM to the culture medium for 30 min at 37ºC. The cells were gently washed once by replacing the medium with bicarbonate (HCO_3^-)-buffered solutions (BBS), and incubated for 10 min prior to experiments in order to allow maximal de-esterification of the dye. The fluorescence of BCECF-AM and Fura-2-AM-loaded cells was measured using MetaFluor®version 6.1 imaging system (Universal Imaging, West Chester, PA). To monitor changes in $[Ca^{2+}]_i$, samples were excited at 340/380 nm and emission was detected at 505 nm; for determination of pH_i in BCECF-AM loaded cells, wavelengths of 440/490 nm and 530 nm were used for excitation and emission, respectively. pH_i values were calculated after calibration using standard methods [27,28].

Electrophysiological recordings

Action potentials (APs) were recorded in TG neurons in whole-cell mode clamp technique using a patch clamp L/M-EPC7 amplifier (HEKA elektronik, Lambrecht, Germany) in conjunction with pClamp 9.2 software and a Digidata 1322A analog-to-digital converter (Axon Instruments, USA). APs were generated by square current pulse injections of 900 pA for 1 sec. The extracellular solution was bicarbonate-buffered solution (BBS; see later in

Methods) and the pipette solution contained (in mM): 125 K gluconate, 10 KCl, 2 $MgCl_2$, 10 EGTA, 10 HEPES. The pH of the pipette solution was adjusted to the desired value with aqueous NaOH.

RT-PCR analysis of NHE1, NBC1, NBC3, NBC4 NDCBE1 and PMCA 1-4

Dissected tissue pieces were ejected into an RNA extraction solution to prepare the RNA and subsequently the cDNA. The PCR primers used to detect the transcripts are shown in Table 1. The conditions used for all PCRs were a hot start of 5 min at 94ºC followed by 35 cycles of 30 sec at 94ºC, 50 sec at 58ºC, and 50 sec at 72ºC. The reactions were terminated with a 7-min incubation at 72ºC and subsequent cooling to 4ºC.

Single-cell RT-PCR

Briefly, single cells were collected by micro pipettes with a tip diameter of about 30 μm. The intracellular contents of a single cell was aspirated into a patch pipette under visual control and was gently put into a reaction tube containing reverse transcription (RT) agents. To avoid genomic DNA contamination, a DNase I digest (40 min at 37ºC) was performed before RT. After heat inactivation, RT was carried out for 50 min at 50ºC (Superscript III, Invitrogen, USA). Subsequently, the cDNA was divided into four or five 2 μl aliquots that were used in separate PCRs. All PCR amplifications were performed with nested primers (Table 2). The first round of PCR was performed in 50 μl of PCR buffer containing 0.2 mM dNTPs, 0.2 μM "outer" primers, 5 μl of RT product, and 0.2 μl of platinum *Taq* DNA polymerase (Invitrogen, USA). The protocol included 5 min of initial denaturation at 95ºC, followed by 35 cycles of 40 sec of denaturation at 95ºC, 40 sec of annealing at

55 ºC, and then 40 sec of elongation at 72 ºC, and was completed with a 7- min final elongation. For the second round of amplification, the reaction buffer (20 μl) contained 0.2 mM dNTPs, 0.2 μM "inner" primers, 5 μl of the products from the first round, and 0.1 μl of platinum *Taq* DNA polymerase. The reaction was the same as the first round. The PCR products were then displayed on the ethidium bromide-stained 2% agarose gel. Gels were photographed using a digital camera.

Small interference RNA (siRNA) design and transfection

The siRNA sequences (GenePharma, Shanghai, China) were as follows: first NHE1 construct, 5'-GCGGCGAGCAGAUCAAUAATT-3' and 5'-UUAUUGAUCUGCUCGCCGCTT-3'; second NHE1 construct, 5'-GAUUCAAGCUCAGCAGCAATT-3' and 5'-UUGCUGCUGAGCUUGAAUCTT-3'; first pNBC1 construct, 5'-GGGCUUCCUUCCUUAAACATT-3' and 5'-UGUUUAAGGAAGGAAGCCCTT-3'; second pNBC1 construct, 5'-GUGUGAUGAAGAAGAAGUATT-3' and 5'-UACUUCUUCUUCAUCACACTT-3'; first PMCA3 construct, 5'-CGAUGGUGUGCUCAUCCAATT-3' and 5'-UUGGAUGAGCACACCAUCGTT-3'; second PMCA3 construct, 5'-GGCUGUGUAGGAGACUAAATT-3' and 5'-UUUAGUCUCCUACACAGCCTT-3'; negative control, 5'-UUCUCCGAACGUGUCACGUTT-3' and 5'-ACGUGACACGUUCGGAGAATT-3'. For transfection, 20 μl of HiPer-Fect transfection reagent (Qiagen Inc., Valencia, CA) and 625 ng of siRNA were combined in DMEM and incubated at room temperature for 15 min. TG

neurons were cleaned of all cell debris and incubated overnight with siRNA/HiPerFect/DMEM at 37ºC. After transfection, TG neurons were moved to normal medium and incubated as described above. TG neuron proteins were homogenized in lysis buffer (50 mM Tris pH 7.5, 1% Triton X-100, 100 mM NaCl, 10 mM tetrasodium pyrophosphate, 10 mM NaF, 1 mM EDTA, 1 mM NaV, 1 mM EGTA, 1 mM phenylmethylsulphonyl fluoride [PMSF] and 1 μg/ml aprotinin, leupeptin and pepstatin) followed by gentle sonification on ice. Following protein concentration determination, the proteins were separated on SDS-polyacrylamide gel and transferred electrophoretically to polyvinylidene fluoride (PVDF) membranes and incubated with NHE1, pNBC1 and PMCA3 antibodies, respectively.

Table 1. List of primer sequences designed for this study

Target gene	Primer sequence	Product size	Genebank no.
Nhe1	5'-ATTCAACAGTGGAGTGACTTGGGTGATGA-3' 5'-GACTGGCAGGGAAGATTCAAAGGGTCTAAA-3'	190 bp	NM_012652
Nhe2	5'-TGACGGTATTAGGGCACAGGTTGGAATGTA-3' 5'- AAATTGGGACAGAGGCGGGGGTAAG-3'	196 bp	NM_012653
Nhe3	5'-CAACGCACCCTAGGAGTTTTAATGCATAGC-3' 5'- TCTCCTCTCAGAATAAGGGTGGCAAACACT-3'	199 bp	M 85300
Nhe4	5'- TCTGAGGGTAGGGATGATTAATTGGTCACA-3' 5'-GCATTGGCCTGTTTCAACATTTCTGA-3'	126 bp	M 85301
Knbc	5'-CACTGAAAATGTGGAAGGGAAG-3' 5'-GACCGAAGGTTGGATTTCTTG-3'	760 bp	NM_003759.3
Pnbc1	5'-CATGTGTGTGACGAAGAAGAAGTAGAAG-3' 5'- GACCGAAGGTTGGATTTCTTG-3'	760 bp	NM_001134742.1
Nbc3	5'-CGGAATTCGTGAACAGCGGGTTAC-3' 5'-GGGCTCATGTTAGGTCTGGTTACT-3'	210 bp	NM_003615.3
Nbc4	5'- GGCTACCATCTGGACCTGTTCTGGGT- '3 5'- CAGTGGATACCGTTTTGGGGATC-3'	750 bp	NM_021196.3
Ndcbe1	5'- GCTCAAGAAAGGCTGTGGCTAC-3' 5'-ACGCCTTAATGACCCAGAGCAG-3'	780 bp	NM_004858.2
Pmca1	5'-GAAAACATCTCCCAATGAAGG-3' 5'-ACCTGAAAGAAGCAAGGGGT-3'	600bp	J03753
Pmac2	5'-GCCTCAAAACCTCTCCTGTT-3' 5'-ATGTCCCCAACCACAATCTC-3'	462 bp	J03754.1
Pmca3	5'-CACAGCCTTCAATGACTG-3' 5'-CCTTCCATGACATGAGTG-3'	399 bp	J05087
Pmca4	5'-AGCGTAGACTTGTTTTTGGG-3' 5'-CCCTTCAATCCAGCCAGTT-3'	233 bp	U15408
Actin	5'- GAGTACAACCTCCTTGCAGCTC-3' 5'- TTGTAGAAAGTGTGGTGCCAAA-3'	350 bp	NM_001148.4

Table 2. DNA primers used for single cell RT-PCR

Target gene	Outer primers	Nested primers	Product size	Genebank no.
Actin	CCC AGA TCA TGT TTG AGA CC AGG ATT CCA TAC CCA GGA AG	AGG CTG TGT TGT CCC TGT AT CAG CTC ATA GCT CTT CTC CA	316 bp	NM_031144
Trpv1	ACC GTC AAC AAG ATT GCA CA TGG TTC CCT AAG CAG ACC AC	TGA CTA CCG GTG GTG TTT CA TGA TCC CTG CAT AGT GTC CA	329 bp	NM_031982
pnbc1	ATG GAG GAT GAA GCT GTC CT GAT ACT GCT GCT GGA CTC AT	GCT TCC TTC CTT AAA CAT GT CCG CAT TCT CCA CAT CAG AT	160 bp	NM_001136260
Nhe1	ATC CCA TCT GCC GTC TCA AC CTC CTC ATT CAC CAG GTC CA	GAA CAT CCA CCC CAA GTC TG CAG TGG GTC TGA GCC TAT GC	298 bp	NM_012652

Materials and solutions

Bicarbonate (HCO_3^-)-buffered solutions (BBS) contained (in mM): 110 NaCl, 5.4 KCl, 1.0 $MgSO_4$, 1.2 $CaCl_2$, 0.4 KH_2PO_4, 0.33 NaH_2PO_4, 20 HEPES, 10 glucose and 25 $NaHCO_3$ (pH 7.4 with NaOH). 4-(2-hydroxyethyl)-1-piperazineethanesulfonic acid (HEPES) buffered solutions (HBS) contained (in mM): 135 NaCl, 5.4 KCl, 0.8 $MgSO_4$, 1.2 $CaCl_2$, 0.4 KH_2PO_4, 0.33 NaH_2PO_4, 20 HEPES, 10 glucose (pH 7.4 with Tris-Base). NH_4^+-containing solutions were prepared by replacing Na^+ with equimolar NH_4^+. During experiments, HBS and BBS solutions were gassed with 100% O_2 and 5% CO_2/95% O_2, respectively. Glutamate and capsaicin were made as stocks in water and ethanol solutions, respectively. 5'-(N-ethyl-N-isopropyl) amiloride (EIPA) and 4',4'-diisothiocyano-stilbene-2',2'-sulfonic acid (DIDS) were made up as stocks in DMSO. All chemicals, unless otherwise stated, were obtained from Sigma (St. Louis, MO). Mouse monoclonal NHE1 antibody, mouse monoclonal PMCA antibody, secondary goat anti-mouse antibody and secondary anti-rabbit antibody were obtained from Santa Cruz (Heidelberg, Germany). Rabbit anti-pNBC1 polyclonal antibody, monoclonal actin antibody and donkey anti-mouse were obtained from Chemicon (Temecula, CA).

Statistical analysis

All data are expressed mean ± SEM unless otherwise stated. Statistical significance was calculated using the Student's unpaired t-test. A probability below 0.05 ($p<0.05$) was considered significant.

3. Results

Identification and distribution of membrane transporters and TRPV1 in TG neurons

I identified the subtypes of NHEs and NBCs in rat TG neurons using reverse-transcriptase polymerase chain reaction (RT-PCR). Bands of 190 bp, 760 bp, 210 bp, 750 bp were detected, corresponding to the predicted sizes for the mRNA transcripts of NHE1, pNBC1, NBC3 and NBC4, respectively (Fig. 1A). On the other hand, transcripts for NHE2, NHE3, NHE4, kNBC1 (kidney type) and Na^+-dependent Cl^-/HCO_3^- exchanger 1 (NDCBE1) were not found in TG neurons. I also examined the expression of TRPV1, NHE1 and pNBC1 in single TG neurons using single-cell RT-PCR (Fig. 1B). mRNA transcripts of NHE1 and pNBC1 were detected in most of the cells I tested (n=8~10 in each experiment), regardless of TG neuron size. However, TRPV1 was detected only in small (<24 μm diameter) and medium sized (24~38 μm diameter) TG neurons. Therefore, the studies on the capsaicin-induced $[Ca^{2+}]_i$ and pH_i change were all performed using small to medium sized TG neurons.

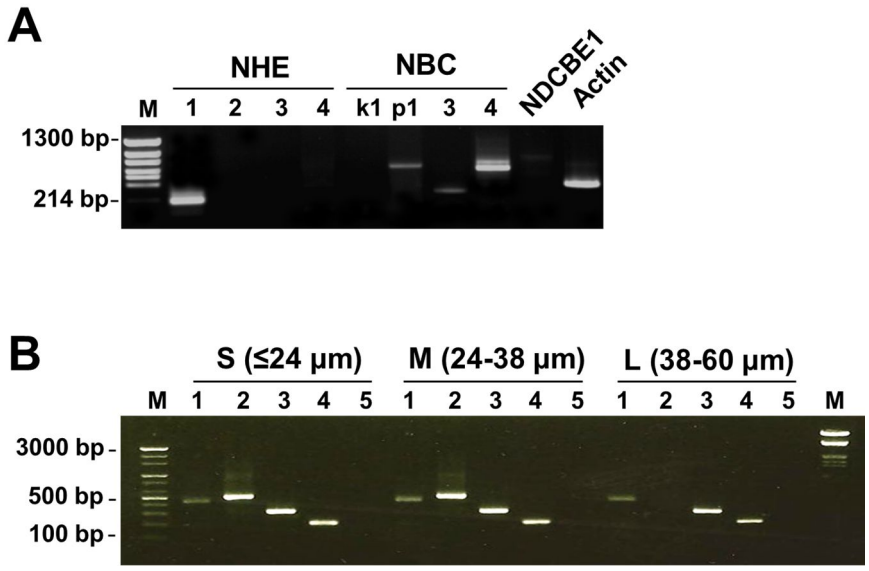
A
NHE
NBC
NDCBE1
Actin
M 1 2 3 4 k1 p1 3 4
1300 bp
214 bp
B
S (≤24 µm)
M (24-38 µm)
L (38-60 µm)
M 1 2 3 4 5 1 2 3 4 5 1 2 3 4 5 M
3000 bp
500 bp
100 bp

Fig. 1. Identification of membrane transporters and TRPV1 in TG neurons **A)** RT-PCR analysis of membrane transporters in whole tissue TG. Primers were selectively designed to detect subtypes of NHE 1, 2, 3, 4 and subtypes of kNBC1 (k1, kidney type), pNBC1 (p1, pancreas type), NBC3, NBC4 and NDCBE1. Actin transcripts were used as the positive control. M: Pwon600 DNA/ECORI+HinfI Digest. Bands of 190 bp, 760 bp, 210 bp, 750 bp were detected, which correspond to the predicted size for the mRNA transcripts of NHE1, pNBC1, NBC3 and NBC4, respectively. **B)** Expression of TRPV1, NHE1 and pNBC1 in single TG neurons using single-cell RT-PCR. TG neurons were divided into small (S), medium (M) and large (L) neurons based on the diameter indicated in parentheses. Lanes 1, 2, 3, 4, and 5 indicates actin, TRPV1, NHE1, pNBC1 and the negative control, respectively. Negative controls were obtained from control pipettes that did not harvest cells but were submerged in bath solution. Predicted product sizes are 329 bp (TRPV1), 298 bp (NHE1), 160 bp (pNBC1), and 316 bp (actin), respectively. Left M: 1 kb DNA ladder, Right M: Lambda/EcoRI+HindIII.

The effects of glutamate and capsaicin on $[Ca^{2+}]_i$ and pH_i in TG neurons

I first examined whether glutamate, one of the main excitatory neurotransmitters, evokes an increase in $[Ca^{2+}]_i$ in rat TG neurons. All $[Ca^{2+}]_i$ and pH_i recordings were performed under the same experimental conditions and time scale: application of glutamate (500 μM) for 1 min at a fixed flow rate of 1.5-2.0 ml/min. The upper panel of Fig. 2A shows a typical $[Ca^{2+}]_i$ response to glutamate. The application of glutamate significantly increased the mean $[Ca^{2+}]_i$ ratio from 0.9 ± 0.01 at rest to 1.4 ± 0.02 (n=5, $p<0.05$). The lower panel of Fig. 2A shows a typical pH_i response to glutamate. The same concentration of glutamate significantly decreased pH_i from 7.35 ± 0.01 at rest to 7.08 ± 0.03 (n=5, $p<0.05$). The rate of the $[Ca^{2+}]_i$ rise was faster than the change in pH_i. The peak $[Ca^{2+}]_i$ (time to peak: 45 ± 0.1 sec, n=5) always preceded the maximal decrease in pH_i (time to peak: 60 ± 0.5 sec, n=5). This result demonstrates that glutamate increases $[Ca^{2+}]_i$ with a concomitant decrease in pH_i. I next studied the effect of capsaicin, an excitatory ligand acting at TRPV1, on $[Ca^{2+}]_i$ and pH_i in TG neurons (Fig. 2B). The pattern of the $[Ca^{2+}]_i$ and pH_i responses to capsaicin was very similar to those of glutamate. Capsaicin (1 μM) increased the $[Ca^{2+}]_i$ ratio from 0.95 ± 0.01 at rest to 1.4 ± 0.27 (n=5, $p<0.05$), and decreased the pH_i from 7.35 ± 0.01 to 7.11 ± 0.01 (n=5, $p<0.05$). As with glutamate application, the $[Ca^{2+}]_i$ peak induced by capsaicin always preceded the maximal change in pH_i. These results suggest that the acidification in TG neurons might be initiated by the rise in $[Ca^{2+}]_i$.

To test this hypothesis, I next examined whether ionomycin and thapsigargin (compounds which increase $[Ca^{2+}]_i$) can mimic the acidification induced by glutamate or capsaicin. Both ionomycin (1 μM) and thapsigargin (5 μM) increased $[Ca^{2+}]_i$ - albeit at a slower rate than glutamate and capsaicin -

followed by a transient decrease in pH_i (Figs. 2C and 2D). The pH_i then recovered to the pre-stimulus level in the presence of ionomycin or thapsigargin. These results suggest that an increase in $[Ca^{2+}]_i$ initiates a transient acidification in TG neurons and that there is a strong pH_i recovery mechanism in these neurons.

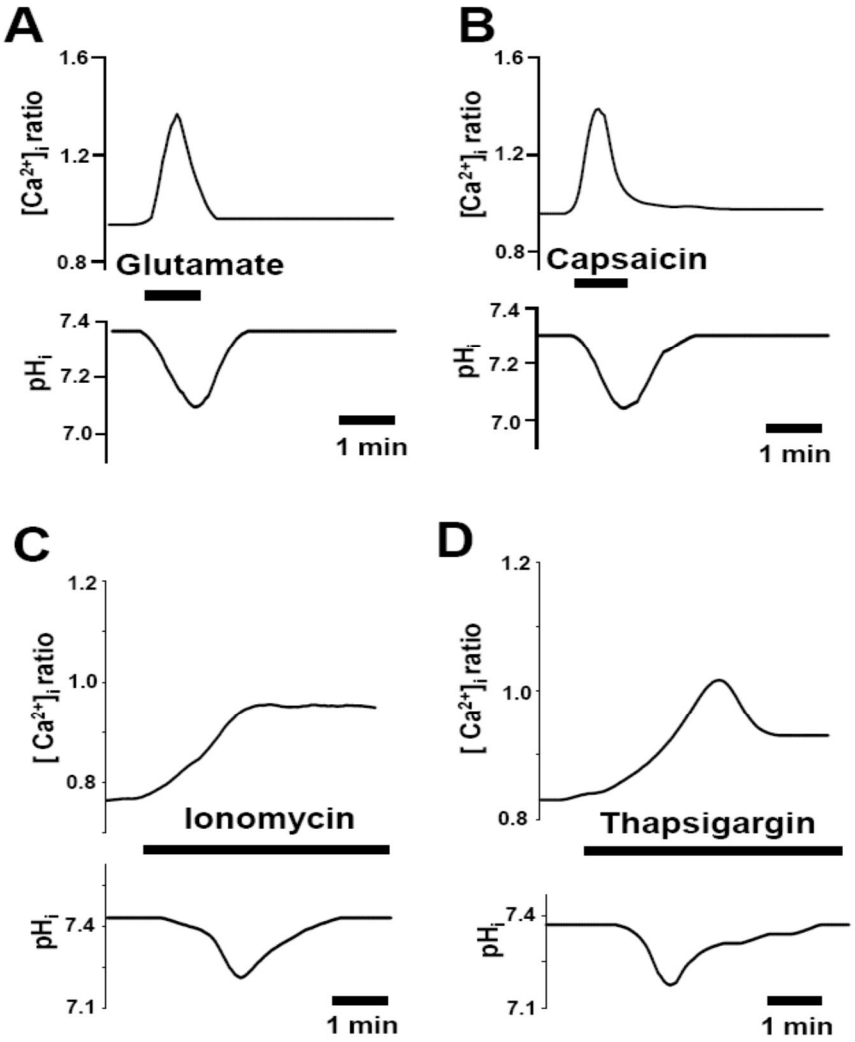
A
1.6
1.2
0.8
[Ca2+]i ratio
Glutamate
7.4
7.2
7.0
pHi
1 min
B
1.6
1.2
0.8
[Ca2+]i ratio
Capsaicin
7.4
7.2
7.0
pHi
1 min
C
1.2
1.0
0.8
[Ca2+]i ratio
Ionomycin
7.4
7.1
pHi
1 min
D
1.2
1.0
0.8
[Ca2+]i ratio
Thapsigargin
7.4
7.1
pHi
1 min

Fig. 2. The effect of glutamate and capsaicin on $[Ca^{2+}]_i$ and pH_i in single TG neurons

Recording of $[Ca^{2+}]_i$ and pH_i was done separately under the same experimental conditions. **A**) A rapid increase of $[Ca^{2+}]_i$ (upper panel) followed by a decrease in pH_i (lower panel) induced by glutamate (500 μM). **B**) A rapid increase in $[Ca^{2+}]_i$ followed by a decrease in pH_i induced by capsaicin (1 μM). **C**) The effects of ionomycin (1 μM) on $[Ca^{2+}]_i$ and pH_i. **D**) The effects of thapsigargin (5 μM) on $[Ca^{2+}]_i$ and pH_i. Each figure is a typical recording from at least 5 experiments. Black bars indicate the period of drug application.

The effect of PMCA inhibitors, $LaCl_3$, on capsaicin and glutamate-induced changes in $[Ca^{2+}]_i$ and pH_i

I next investigated the mechanism underlying the Ca^{2+}-induced acidification in TG neurons. The PMCA was a strong candidate for mediating intracellular acidification in response to a rise in $[Ca^{2+}]_i$. Thus, I examined the effect of $LaCl_3$, a general PMCA inhibitor, on the glutamate and capsaicin-induced changes in $[Ca^{2+}]_i$ and pH_i. TG neurons were pretreated with $LaCl_3$ (1 mM) for 5 min prior to glutamate application. Fig. 3A shows superimposed recordings of the glutamate-induced $[Ca^{2+}]_i$ increase before (solid line) and after (dotted line) $LaCl_3$ treatment (upper panel). Neither the rate nor the magnitude of the glutamate-induced $[Ca^{2+}]_i$ rise was affected by $LaCl_3$ pretreatment. However, $[Ca^{2+}]_i$ did not return to the pre-stimulus level in the $LaCl_3$ pretreated group. This sustained $[Ca^{2+}]_i$ level was 21 ± 3% (n=5) higher than the basal level, suggesting that $LaCl_3$ partly inhibits Ca^{2+} efflux via PMCA. I also examined the effects of $LaCl_3$ on the glutamate-induced acidification (lower panel of Fig. 3A). $LaCl_3$ reduced the magnitude of the glutamate-induced pH_i decrease by 50 ± 1%. The rate of the acidification was 0.22 ± 0.012 pH units/min in control (solid line), which fell to 0.12 ± 0.01 pH units/min (n=5) after $LaCl_3$ treatment (dotted line). The inhibitory effects of $LaCl_3$ on the capsaicin-induced $[Ca^{2+}]_i$ and pH_i change were very similar to those of glutamate (Fig. 3B; upper and lower panels, respectively).

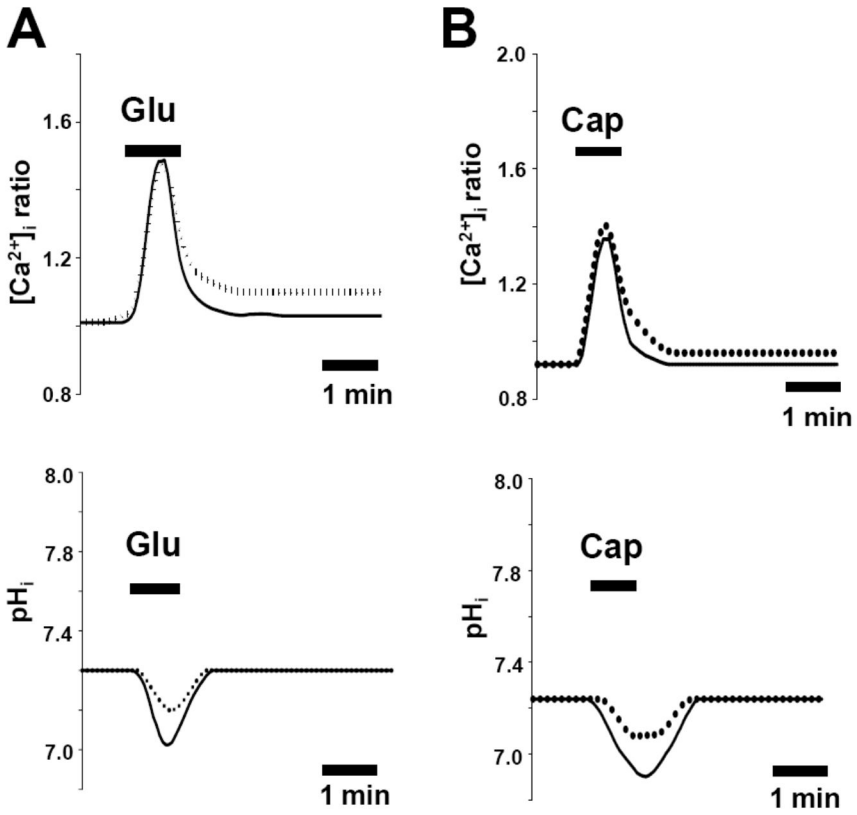
A
B
Glu
Cap
1.6
1.2
0.8
2.0
$[Ca^{2+}]_i$ ratio
1 min
8.0
7.8
7.4
7.0
pH_i

Fig. 3. The effects of $LaCl_3$ on $[Ca^{2+}]_i$ and pH_i evoked by glutamate or capsaicin stimulation in TG neurons

$LaCl_3$ (1 mM) was applied to the recording chamber for 5 min before the TG stimulation with glutamate or capsaicin. **A)** Glutamate (500 μM) induced an increase in $[Ca^{2+}]_i$ (upper panels) and a decrease in pH_i (lower panels) in control (solid line) and in the presence of $LaCl_3$ (1 mM) (dotted lines). $LaCl_3$ did not affect the increase in $[Ca^{2+}]_i$ but did prevent $[Ca^{2+}]_i$ recovery. The sustained $[Ca^{2+}]_i$ level (dotted line) was higher than the basal level. $LaCl_3$ also partially blocked the pH_i decrease (lower panels in Fig. 3A). **B)** The inhibitory effect of $LaCl_3$ on the capsaicin-induced $[Ca^{2+}]_i$ and pH_i change was very similar to that of glutamate.

The effect of PMCA inhibitors, O-vanadate , on capsaicin and glutamate-induced changes in $[Ca^{2+}]_i$ and pH_i

I performed additional studies with another PMCA inhibitor, O-vanadate. The inhibitory effect of O-vanadate (10 mM) was tested on the capsaicin-induced $[Ca^{2+}]_i$ and pH_i change. Fig. 4A shows that application of O-vanadate delays the reduction in $[Ca^{2+}]_i$ after capsaicin (1 μM) application and sustains $[Ca^{2+}]_i$ at a higher level than the resting state level (the second and third peak in Fig. 4A). Fig. 4B shows the pH_i decrease by capsaicin alone (Cap) and in the presence of O-vanadate (Cap+Va). Acidification by capsaicin was almost completely inhibited by O-vanadate (96 ± 0.01%, n=3). I performed a similar experiment in Ca^{2+}-free medium. Fig. 4C and 4D shows the change in $[Ca^{2+}]_i$ and pH_i induced by capsaicin in Ca^{2+}-free medium. Neither the $[Ca^{2+}]_i$ increase nor acidification was observed when capsaicin was applied in Ca^{2+}-free medium.

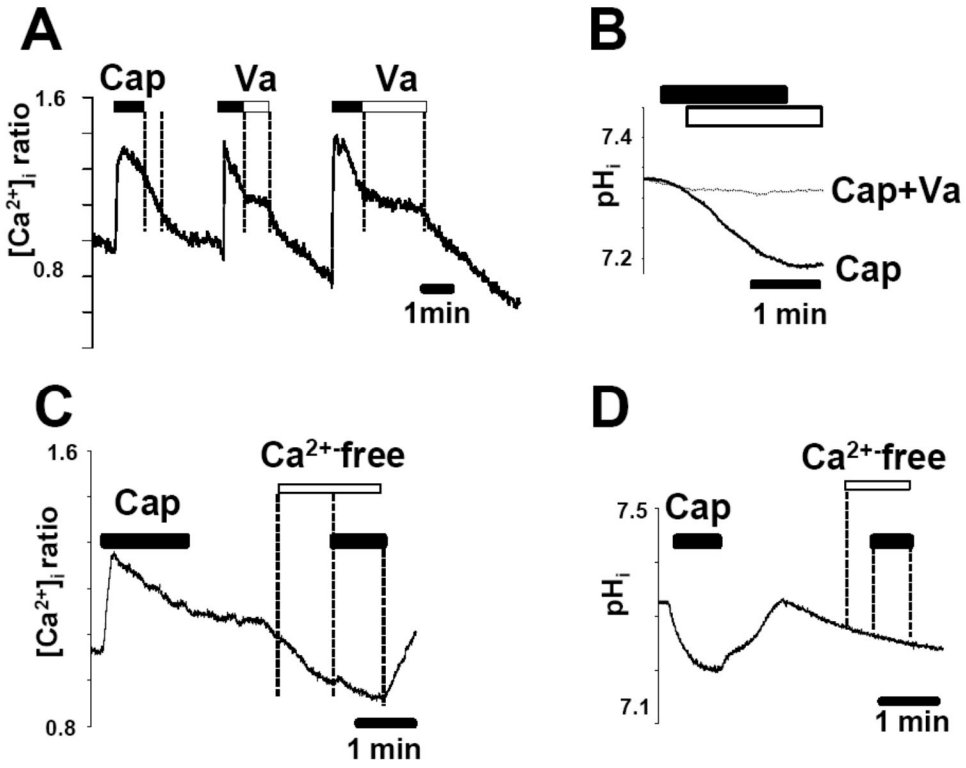
A
Cap
Va
Va
1.6
0.8
[Ca2+]i ratio
1min
B
7.4
7.2
pHi
Cap+Va
Cap
1 min
C
1.6
0.8
[Ca2+]i ratio
Cap
Ca2+-free
1 min
D
7.5
7.1
pHi
Cap
Ca2+-free
1 min

Fig. 4. Inhibitory effects of PMCA inhibitors on the capsaicin-induced changes in $[Ca^{2+}]_i$ and pH_i

A) Effect of O-vanadate (10 mM; Va) on $[Ca^{2+}]_i$ after capsaicin (1 μM; Cap). The $[Ca^{2+}]_i$ level was sustained during the application of O-vanadate (the second and third peak) compared to control. **B)** Effect of O-vanadate (10 mM; Va) on pH_i. Application of O-vanadate after capsaicin (Cap+Va) completely inhibited the pH_i decrease compared to capsaicin alone (Cap). Black and white bars represent duration of capsaicin and O-vanadate application, respectively. **C)** and **D)** The effect of capsaicin (Cap, black bar) on $[Ca^{2+}]_i$ and pH_i in Ca^{2+}-free medium. Neither the increase in $[Ca^{2+}]_i$ nor decrease of pH_i was observed in Ca^{2+}-free medium.

Identification and effect of PMCA3 in TG neuron

I identified the subtypes of PMCA in whole TG using RT-PCR. Bands of 600 bp, 462 bp and 399 bp were detected, which correspond to the predicted size for the mRNA transcripts of PMCA1, 2, and 3, respectively (Fig. 5A). On the other hand, transcripts for PMCA4 (233 bp) were not found in TG. I further examined the expression of PMCA subtypes in visually identified single TG neurons using single-cell RT-PCR (Fig. 5B). mRNA transcripts for PMCA3 (lane 3) were detected in most cells tested (n=8~10 in each experiment) regardless of TG neuron size. PMCA1 was detected only in large TG neurons (38-60 μm diameter). However, PMCA2 was not detected in any TG neurons. Based on these data I next studied whether PMCA3 was involved in the capsaicin-induced $[Ca^{2+}]_i$ and pH_i change by using an siRNA knockdown approach. All siRNA experiments were performed on small to medium sized neurons throughout. Fig. 5C shows the capsaicin-induced pH_i decrease after treatment with PMCA3 siRNA compared to control. Acidification by capsaicin was almost completely inhibited by PMCA3 siRNA (96 ± 0.01%, n=3). Western blot analysis showed that transfection of cultured TG cells with PMCA3 siRNA reduced PMCA3 expression by 60 ± 0.01% (n=3), where as PMCA3 control siRNA did not significantly affect PMCA3 expression (Fig 5D). The experiment was repeated with a second PMCA3 siRNA construct which reduced PMCA3 expression by 52 ± 0.01% (n=3; data not shown). These results indicate that the capsaicin-induced changes in $[Ca^{2+}]_i$ and pH_i in small and medium-sized TG neurons are dependent on the activity of PMCA3 specifically.

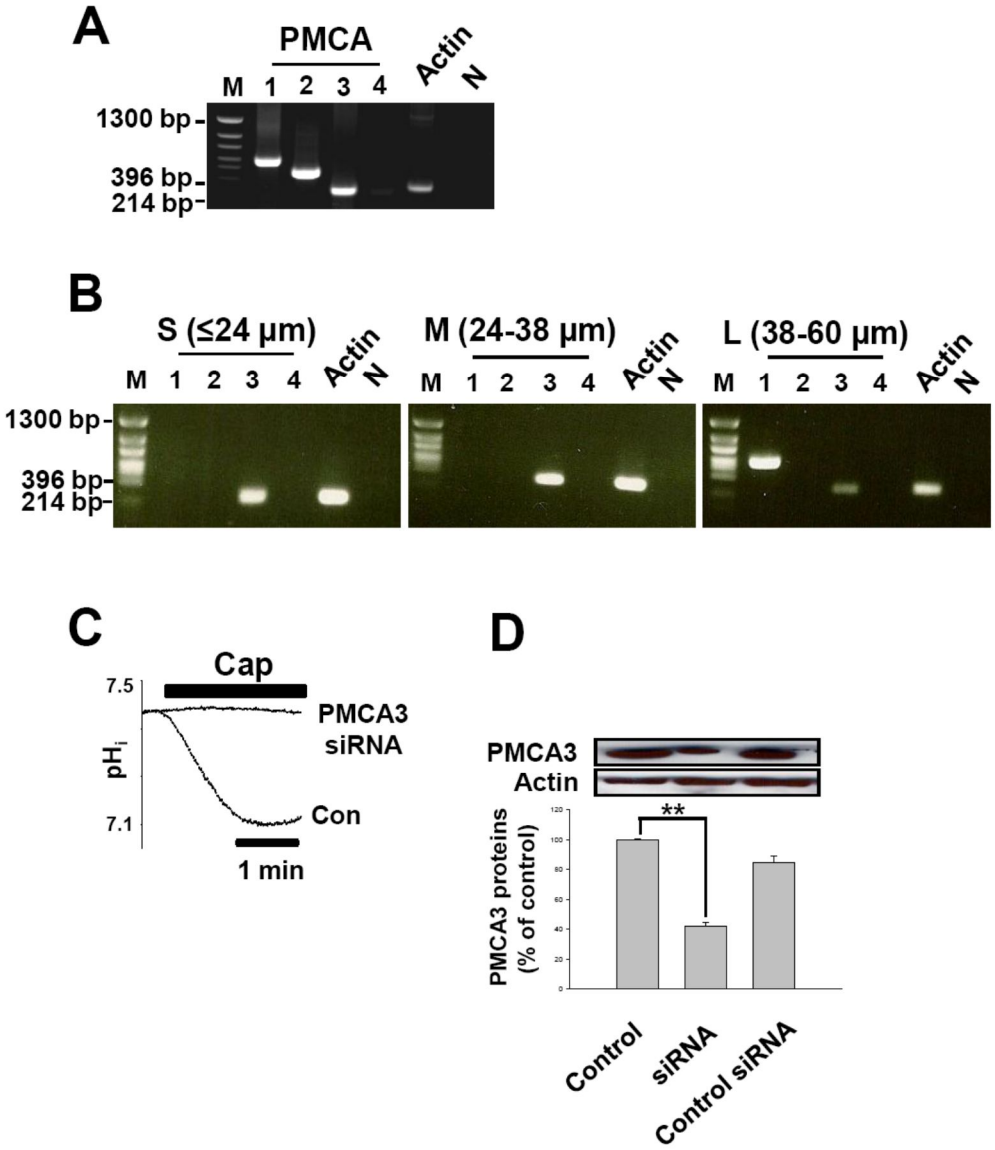
A
PMCA
M 1 2 3 4
Actin N
1300 bp
396 bp
214 bp
B
S (≤24 μm)
M (24-38 μm)
L (38-60 μm)
M 1 2 3 4
Actin N
1300 bp
396 bp
214 bp
C
Cap
7.5
pHi
7.1
PMCA3 siRNA
Con
1 min
D
PMCA3
Actin
**
PMCA3 proteins (% of control)
Control
siRNA
Control siRNA

Fig. 5. Inhibitory effects of PMCA3 siRNA on the capsaicin-induced changes in $[Ca^{2+}]_i$ and pH_i

A) RT-PCR analysis of membrane transporters in whole tissue TG. Primers were selectively designed to detect the subtypes of PMCA 1, 2, 3 and 4. Actin transcripts were used as the positive control (316 bp). M: Pwon600 DNA/*ECORI*+*HinfI* Digest. Bands of 600 bp, 462 bp, and 399 bp were detected, which correspond to the predicted size for the mRNA transcripts of PMCA1, 2 and 3 (lanes 1, 2 and 3), respectively. Transcripts for PMCA4 (233 bp, lane 4) were not found. N: negative control. **B)** Expression of PMCA subtypes in single TG neurons using single-cell RT-PCR. TG neurons were divided into small (S), medium (M) and large (L) neurons based on the diameter indicated in parentheses. **C)** Effect of PMCA3 siRNA on pH_i. Cells pre-transfected with PMCA3 siRNA after capsaicin nearly completely inhibited the pH_i decrease. **D)** The knock-down effect of PMCA3 siRNA in TG neurons. TG neurons transfected with a first PMCA3 construct siRNA and control siRNAs for 16 hrs were incubated in DMEM media prior to the extraction of proteins for Western blots of PMCA3 and actin. The data are presented as mean ± SEM (n=3). **$p<0.01$ vs. control.

Identification of membrane transporters in TG neurons involved in the pH_i recovery from intracellular acidification.

My results thus far have demonstrated that there is a robust pH_i recovery mechanism in TG neurons. Next I investigated the kinds of membrane transporters involved in the pH_i recovery from intracellular acidification. For this experiment I used an NH_4Cl pulse technique in which exposure to NH_4Cl (20 mM) for 1 min induces a transient alkalization followed by intracellular acidification [24]. I then measured the rate of pH_i recovery with and without HCO_3^- in the extracellular solution, as well as in the presence of specific transporter blockers. In some experiments, NH_4Cl pulse was followed by Na^+ free bath solution to examine the Na^+ dependency of the transporter function. Fig. 6A shows the pH_i recovery pattern in TG neurons after NH_4Cl application. The pH_i recovery rate was significantly higher in a HCO_3^--buffered solution (BBS)(0.270 ± 0.009 pH units/min; n=5, $p<0.05$) than in a HEPES-buffered solution (HBS)(0.125 ± 0.014 pH units/min, n=5). Fig. 6B shows the pH_i recovery rate from cell acidification in HBS. Application of 5 μM 5'-(N-ethyl-N-isopropyl) amiloride (EIPA), a specific blocker for NHE1, completely blocked the pH_i recovery (Fig. 6B). I then investigated the pH_i recovery in BBS. EIPA only partially inhibited pH_i recovery in the presence of HCO_3^- (0.165 ± 0.003 pH units/min, n=5). pH_i recovery was not observed when Na^+ was absent from the extracellular medium. The pH_i recovery component remaining in the presence of EIPA (0.105 ± 0.002 pH units/min, n=5) was completely inhibited by the addition of 4',4'-diisothiocyano-stilbene-2',2'-sulfonic acid (DIDS; 500 μM), an inhibitor of pNBC1 (Fig. 6D). These results suggest that in addition to NHE1, TG neurons also possess functional pNBC1, which is EIPA-insensitive

and dependent of the presence of Na^+ and HCO_3^- ions. The mean pH_i recovery rates in each experimental condition are summarized in Fig. 6E.

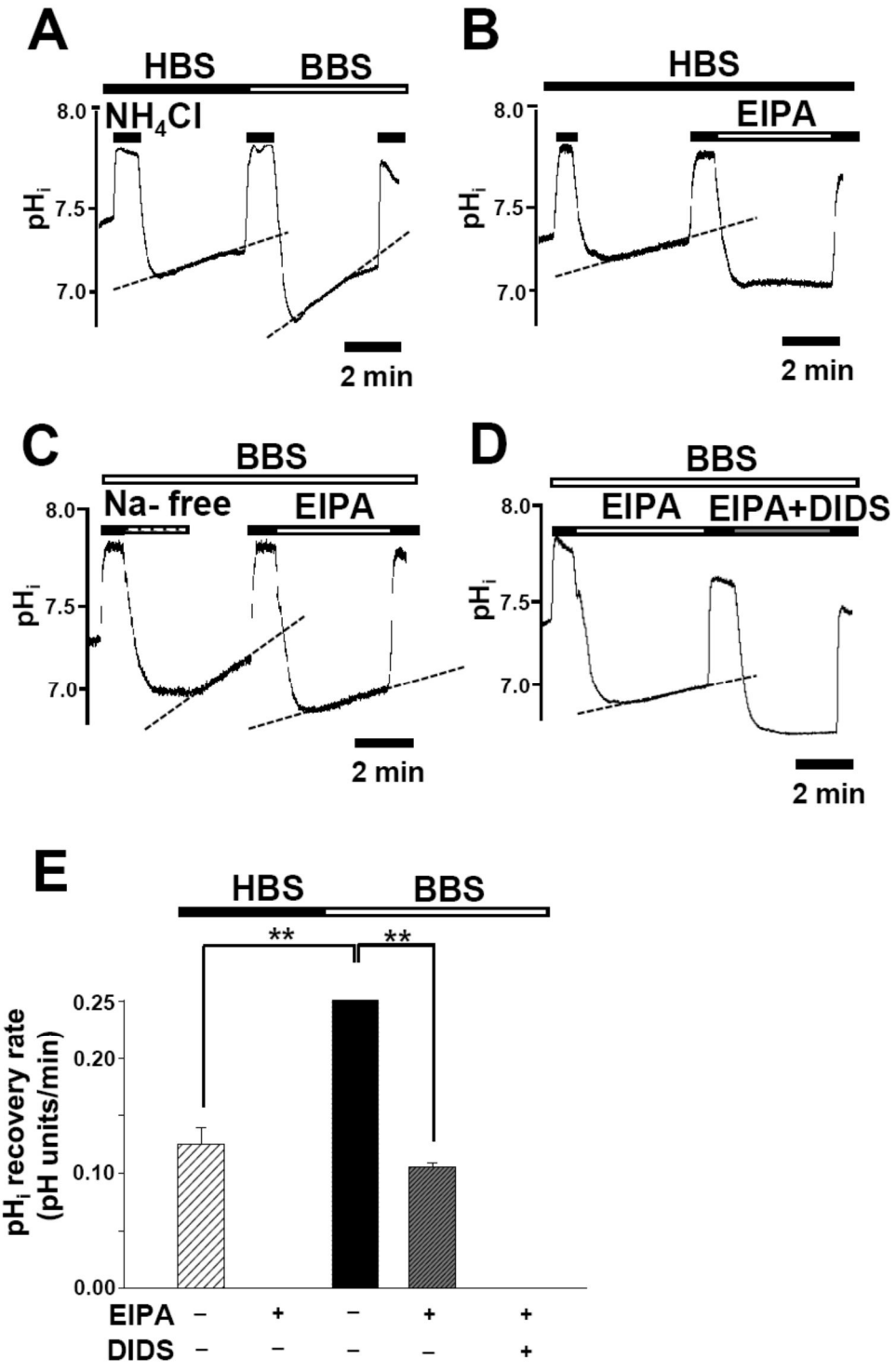
A
HBS
BBS
NH4Cl
8.0
7.5
7.0
pHi
2 min
B
HBS
EIPA
8.0
7.5
7.0
pHi
2 min
C
BBS
Na- free
EIPA
8.0
7.5
7.0
pHi
2 min
D
BBS
EIPA
EIPA+DIDS
8.0
7.5
7.0
pHi
2 min
E
HBS
BBS
**
**
pHi recovery rate
(pH units/min)
0.25
0.20
0.10
0.00
EIPA – + – + +
DIDS – – – – +

Fig. 6. The pH_i recovery of TG neurons from acidification induced by NH_4Cl pulse

A) Normal pH_i recovery in HEPES-buffered solutions (HBS) and bicarbonate-buffered solutions (BBS). Note the faster pH_i recovery in BBS than in HBS. **B**) A complete inhibition of the pH_i recovery in the presence of EIPA (5 μM) in HBS. **C**) Inhibition of pH_i recovery in Na^+-free bath solution and the partial inhibition of pH_i recovery in the presence of EIPA (5 μM) in BBS. **D**) Complete inhibition of pH_i recovery in the presence of both EIPA (5 μM) and DIDS (500 μM) in BBS. **E)** A summary of the result showing the average pH_i recovery rates in TG neurons in the presence of specific inhibitors, EIPA and/or DIDS, in HBS or BBS. The data are presented as mean ± SEM (n=5). **$p<0.01$.

Inhibitory effects of NHE1 and pNBC1 siRNA in TG neurons

I further confirmed the role of NHE1 and pNBC1 using a knockdown approach. Fig. 7A shows the normal pH_i recovery pattern in TG neurons transfected with control siRNA. The pattern of pH_i recovery from acidification was very similar to that of the non-treated group (Fig. 6A). The pH_i recovery rate in control siRNA transfected cells was also higher in BBS than in HBS, suggesting that both NHE1 and pNBC1 were functioning normally. Transfection of cultured TG neurons with NHE1 siRNA completely inhibited pH_i recovery in HBS, while a pH_i recovery component remained in BBS (Fig. 7B), possibly mediated by pNBC1. After transfection with siRNA for pNBC1, the pH_i recovery in the presence of HBS (Fig. 7C) was similar to that in control (Fig. 7A). However, siRNA knockdown of pNBC1 did slow the pH_i recovery rate in BBS (Fig. 7C) compared to control siRNA (Fig. 7A). The remaining pH_i recovery component may due to the residual function of NHE1.

Western blot analysis showed that transfection of TG neurons with NHE1 and pNBC1 siRNA markedly reduced the expression of NHE1 (66 ± 0.01%, n=3) and pNBC1 (46 ± 0.01%, n=3), respectively (Fig. 7D and E). Transfection of TG neurons with second constructs for NHE1 and pNBC1 siRNA also resulted in a marked inhibition of the NHE1 (25 ± 0.05%, n=3) and pNBC1 proteins (65 ± 0.01%, n=3) (data not shown), further confirming the specificity of NHE1 and pNBC1 siRNA for NHE1 and pNBC1 knockdown, respectively. Pretreatment with either control siRNA construct did not significantly affect NHE1 and pNBC1 expression (lane 3 in Fig. 7D and E). These results further confirm that NHE1 and pNBC1 play key roles in pH_i regulation in TG neurons.

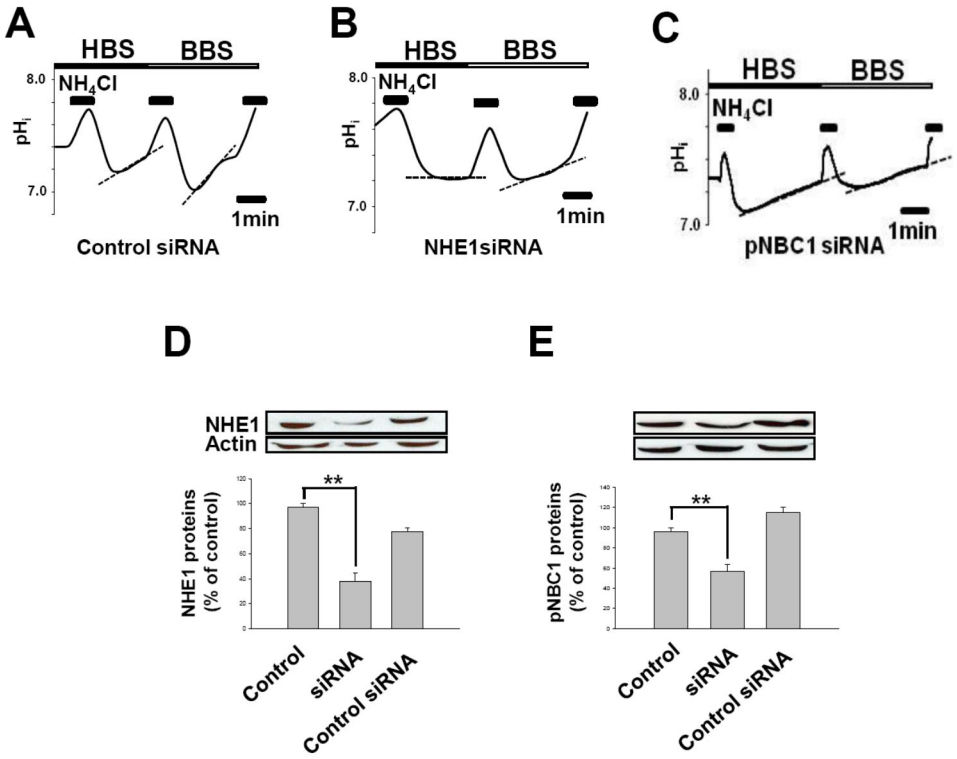
A
HBS
BBS
8.0
NH4Cl
pHi
7.0
1min
Control siRNA
B
HBS
BBS
8.0
NH4Cl
pHi
7.0
1min
NHE1siRNA
C
HBS
BBS
8.0
NH4Cl
pHi
7.0
1min
pNBC1 siRNA
D
NHE1
Actin
NHE1 proteins
(% of control)
**
Control
siRNA
Control siRNA
E
pNBC1 proteins
(% of control)
**
Control
siRNA
Control siRNA

Fig. 7. pH_i recovery in TG neurons transfected with control siRNA, NHE1 siRNA and pNBC1 siRNA

A) A normal pH_i recovery pattern was observed in TG neurons transfected with control siRNA. **B**) Transfection of TG neurons with NHE1 siRNA completely inhibited pH_i recovery in HBS. However in BBS a pH_i recovery component remained, possibly mediated by pNBC1. **C)** Transfection of TG neurons with pNBC1 siRNA in BBS (right) shows a similar pH_i recovery rate compared to that in HBS (left), possibly mediated by NHE1. **D)** The effect of NHE1 siRNA knock-down in TG neurons. Western blot analysis showed that transfection of TG neurons with the first NHE1 construct siRNA (but not control siRNA) resulted in a marked inhibition of NHE1 expression. **E)** The effect of pNBC1 siRNA knock-down. Transfection of TG neurons with the first pNBC1 construct siRNA (but not control siRNA) resulted in a marked inhibition of pNBC1 expression.

Modulation of action potentials (APs) in TG neurons by pH_i

I next examined whether pH_i can affect the excitability of TG neurons by again employing the NH_4Cl pulse technique. I have already shown that an NH_4Cl pulse induces two different pH_i states in TG neurons: a transient cell alkalization (~1 min) followed by cell acidification after washout of NH_4Cl (see inset in Fig. 8). APs were elicited in TG neurons with a current injection of 900 pA for 1 sec in BBS using current-clamp technique. Fig. 8A shows the firing pattern in a TG neuron before NH_4Cl pulse (4 ± 0.1 APs/sec; n=5). During the early phase of the NH_4Cl pulse (Fig. 8B), which corresponds to cell alkalization, the frequency of APs was significantly increased (11 ± 0.5 APs/sec, n=5; $p<0.05$). After washout of NH_4Cl (Fig. 8C), AP frequency was markedly decreased (3 ± 0.5 APs/sec; n=5, $p<0.05$). Seven minutes after washout (Fig. 8D), the AP frequency recovered to that of control (4 ± 0.5 APs/sec; n=5). The effect of pH_i on AP frequency was further confirmed by directly changing the pH of the recording patch pipette solution. AP frequency was significantly lower (2 ± 0.5 APs/sec, n=5, $p<0.05$) with a pipette solution of pH 6.8 (Fig. 8E). In contrast, AP frequency was significantly higher (19 ± 0.5 APs/sec, n=5, $p<0.01$) with a pipette solution of pH 7.8 (Fig. 8F).

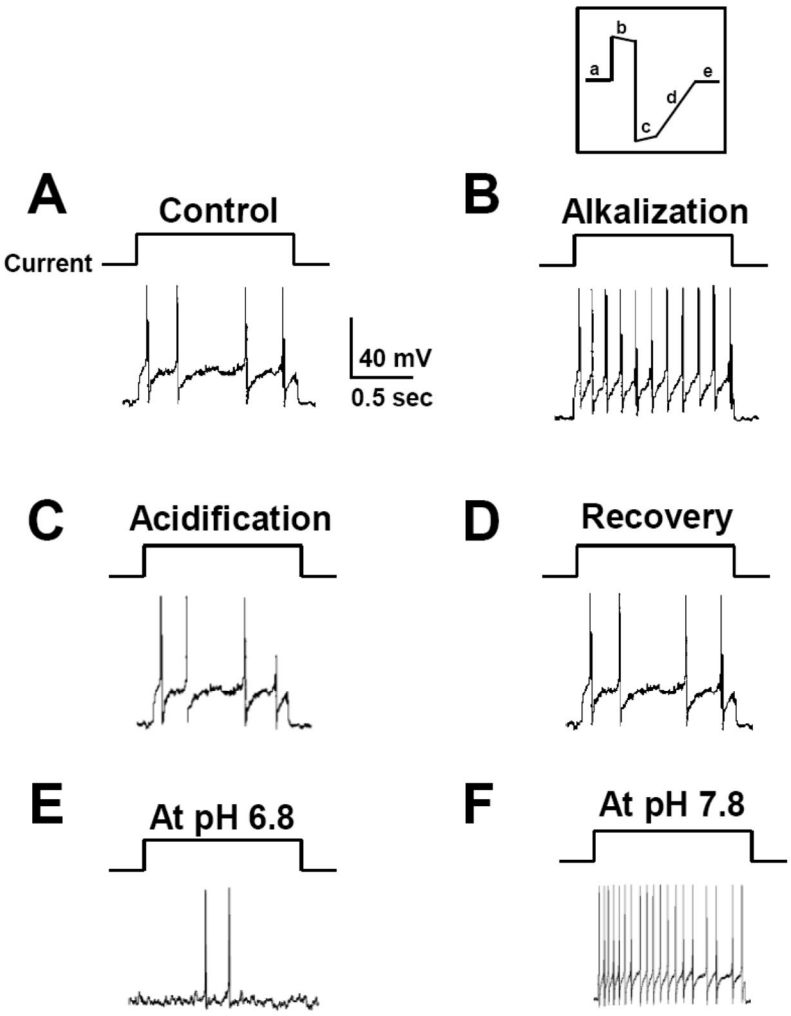
a
b
c
d
e
A
Control
Current
40 mV
0.5 sec
B
Alkalization
C
Acidification
D
Recovery
E
At pH 6.8
F
At pH 7.8

Fig. 8. The effect of pH_i on the frequency of action potentials (AP) in TG neurons in BBS

The inset shows pH_i status induced by NH_4Cl (20 mM) pulse; "b", "c" and "d" indicates cell alkalization, acidification and pH_i recovery periods, respectively. **A**) APs in response to a 900 pA current injection for 1 sec in control ("a" on the inset). **B**) The increase in AP frequency during the alkalization periods ("b" on the inset). **C**) APs 2 min after washout of NH_4Cl, which equates to the acidification period ("d" on the inset). **D**) APs 7 min after washout of NH_4Cl (e in the inset). pH_i had recovered to baseline in this period. **E** and **F**) AP frequency with pipette solutions of pH 6.8 and 7.8, respectively. In Figs A-D, the pH of the pipette solution was adjusted to 7.4.

The effect of EIPA and/or DIDS on action potentials (AP) in TG neurons

Finally, I examined whether the inhibition of membrane transporters NHE1 and pNBC1 can directly contribute to the modulation of AP frequency in BBS during pH_i recovery. Fig. 9 shows current-clamp recordings of a TG neuron during pH_i recovery periods, which corresponds to the periods of "D" in the inset of Fig. 8. Application of EIPA (5 μM) or DIDS (500 μM) significantly decreased AP frequency to 3 ± 0.1 APs/sec (n=5, $p<0.05$) and to 2 ± 0.1 APs/sec (n=5, $p<0.05$), respectively, compared to control (4 ± 0.1 APs/sec; n=5) (Fig. 9A and 9B). The simultaneous application of both inhibitors further reduced the AP frequency (1 ± 0.5APs/sec, n=5, $p<0.01$) (Fig. 9C). These results are summarized in Fig. 9D. My data has shown that AP frequency in TG neurons is dependent on pH_i, and that EIPA and DIDS prolong cell acidification by blocking NHE1 and pNBC1 transporters, respectively.

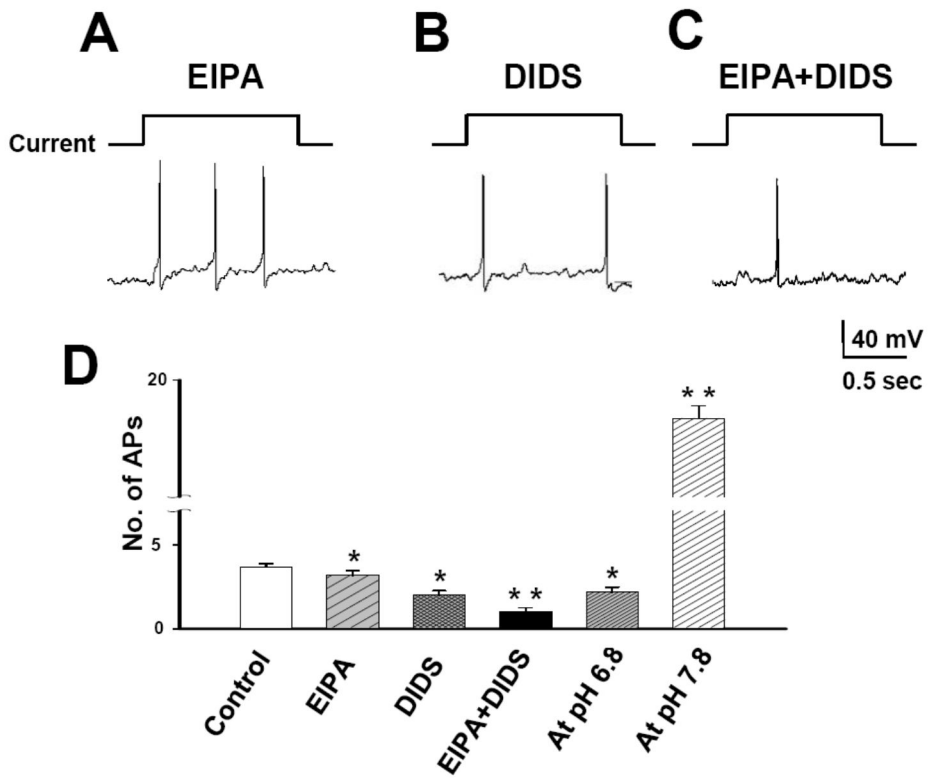
A
EIPA
B
DIDS
C
EIPA+DIDS
Current
40 mV
0.5 sec
D
No. of APs
20
5
0
* *
*
*
* *
*
* *
Control
EIPA
DIDS
EIPA+DIDS
At pH 6.8
At pH 7.8

Fig. 9. The effect of EIPA and/or DIDS on AP frequency in TG neurons in BBS

A) APs in response to a 900 pA current injection for 1 sec in the presence of EIPA (5 μM), a specific NHE1 inhibitor. The frequency of APs was significantly decreased compared to the control. **B)** APs in the presence of DIDS (500 μM), a non-specific NBC1 inhibitor. The frequency of APs was also significantly decreased compared to control. **C)** APs in the presence of both EIPA and DIDS. The simultaneous application of both inhibitors further reduced AP frequency. **D)** A summarized result quantifying the effect of EIPA and/or DIDS and intracellular pH on AP frequency (*$p<0.05$ and **$p<0.01$).

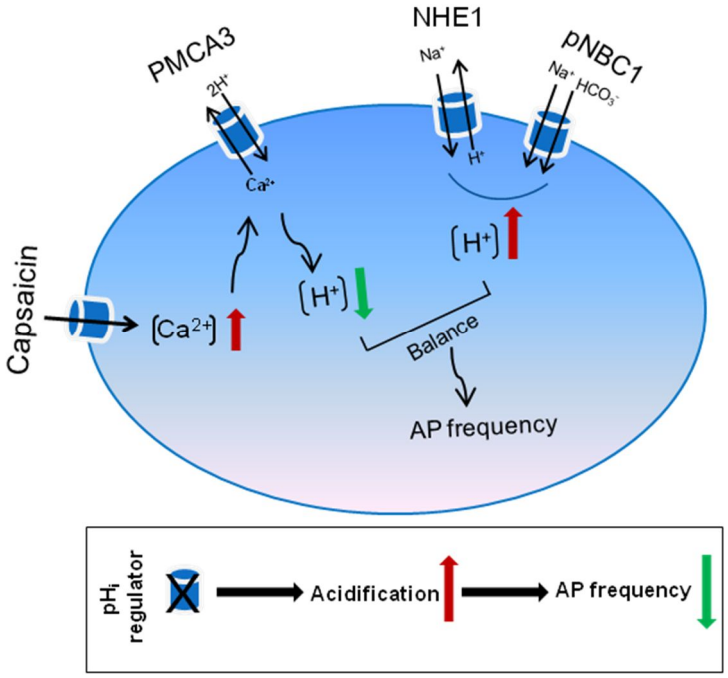
NHE1
PMCA3
pNBC1
Na+
2H+
Na+ HCO3-
Ca2+
H+
Capsaicin
[H+]
[Ca2+]
[H+]
Balance
AP frequency
pHi regulator
Acidification
AP frequency

Fig. 10. Schematic diagram of pH regulation mechanism in trigeminal ganglion

Various neurotransmitters including capsaicin increase intracellular calcium. As calcium elevates, PMCA3 intrudes calcium in exchange for hydrogen, resulting in acidification. To maintain pH homeostasis, NHE1 and pNBC1involved pH recovery mechanism are significantly activated. NHE1 exchanges extracellular sodium and intracellular hydrogen. pNBC1 cotransports sodium and bicarbonate into cytosol. In addition, acidification of cells induced by NHE1 and pNBC1 inhibition decreases AP frequency. This implys that change of intracellular ph crucially modulates AP frequency.

4. Discussion

The levels of intracellular Ca^{2+} and pH play vital roles in sensory neurons including synaptic plasticity, neurotransmitter release and gene regulation [29]; even subtle changes to $[Ca^{2+}]_i$ and pH_i may have drastic physiological or pathological consequences [5]. Several mechanisms of Ca^{2+}-induced intracellular acidification have been proposed in a number of cell types [11,16,17,28]. Neurotransmitters may also induce intracellular acidification through mechanisms that involve elevation of $[Ca^{2+}]_i$ [30].

In this study, both glutamate and capsaicin were able to induce concomitant changes in $[Ca^{2+}]_i$ and pH_i. Removal of extracellular Ca^{2+} completely blocked the acidification induced by capsaicin, showing that the influx of Ca^{2+} is both necessary and sufficient to induce intracellular acidification by neurotransmitter receptor activation. I found that TRPV1, the receptor activated by capsaicin, was expressed only in small and intermediate sized TG neurons that are thought to be nociceptive [31]. Glutamate has been shown to sensitize mechanosensitive afferents [32] and capsaicin has been shown to activate and sensitize trigeminal afferents; TRPV1 may also mediate Ca^{2+}-dependent intracellular acidification in DRG neurons [10]. Thus, both glutamate and capsaicin may possibly modulate the processing of nociceptive input in TG neurons from craniofacial tissues [33] via mechanisms involving $[Ca^{2+}]_i$ elevation and pH_i acidification.

While the PMCA is primarily involved in Ca^{2+} regulation, it may also play a secondary role in pH_i regulation in the process of extruding Ca^{2+} [15,16]. The PMCA appears to be responsible for the recovery of physiological Ca^{2+} levels and intracellular acidification by counter-transport of H^+ in vascular smooth muscle cells (10) and neurons [34]. In cerebellar granule cells [15] and

pancreatic acini (13) $LaCl_3$ inhibits Ca^{2+}-ATPases at the plasma membrane and endoplasmic reticulum (ER), both of which are known to operate as Ca^{2+}/H^+ exchangers. Thus, I tested the effect of $LaCl_3$ on the Ca^{2+}-induced acidification evoked by capsaicin in TG neurons. My data showed that $LaCl_3$ reduced the level of acidification after the capsaicin-induced $[Ca^{2+}]_i$ elevation. I performed an additional study with another PMCA inhibitor, O-vanadate, which has been shown to completely block PMCA activity in cerebellar granule cells (28). O-vanadate showed a stronger inhibition of the PMCA activity than $LaCl_3$ in TG neurons. O-vanadate prevented the return of $[Ca^{2+}]_i$ to baseline after capsaicin, and in doing so completely blocked acidification. These data indicate that acidification is at least partly due to Ca^{2+}/H^+ exchange through the PMCA (Fig. 3).

To date, several possible mechanisms have been proposed to account for Ca^{2+}-induced intracellular acidification in neurons and other cell types [35]. These include overproduction of CO_2/lactate, and collapse of the mitochondrial membrane potential due to Ca^{2+} uptake [11]. I identified the expression of PMCA subtypes in TG neurons and found that PMCA3 was expressed in all TG neurons, regardless of size (Fig 5B). Together my results strongly suggested that the PCMA subtype, PMCA3, is the main contributor to the $[Ca^{2+}]_i$-induced acidification in response to neurotransmitter receptor activation in TG neurons.

Ion and pH homeostasis in neurons is regulated by various acid-base transporters, for example the NHE family and the HCO_3^--dependent acid-base transport protein family [36,37]. In particular, the NHE subtype 1 (NHE1), NDCBE, AE3, and NBC are key contributors to acid-base regulation in neurons [5]. NHE1 and pNBC1 were functionally expressed in TG neurons of all sizes and the activities of both were dependent on the presence of extracellular Na^+.

The specific NHE1 inhibitor, EIPA, blocked pH_i recovery in HBS demonstrating the function of NHE1 in TG neurons. The NBC family includes the electrogenic Na^+-HCO_3^- co-transporter (NBC1 and NBC4) and electro-neutral Na^+-HCO_3^- co-transporter (NBC3) as well as Na^+-dependent Cl-HCO_3^- exchange (NDCBE) [38]. In my experiments, mRNA transcripts of NBC1, NBC3 and NBC4 were detected in TG neurons. DIDS, a non-specific blocker for NBC1, together with EIPA, completely inhibited pH_i recovery of TG neurons in BBS. However, I cannot rule out the possibility that other non-DIDS sensitive NBCs also contribute to the pH_i recovery. Unfortunately, specific inhibitors for NBC3 or 4 are not yet available. Nevertheless, the complete inhibition of pH_i recovery by DIDS strongly suggests that NBC1 is a main contributor to pH_i recovery among the NBC family in HCO_3^--buffered solutions.

NBC1 has two variants: kNBC1 from kidney, and pNBC1 from pancreas. I found that the NBC1 expressed in TG neurons is the pancreatic type, which has been reported in pancreas [39,40] and salivary glands [41,42]. I further confirmed the role of NHE1 and pNBC1 in pH_i recovery by treating TG neurons with siRNA. There was a substantial loss of pH_i recovery function after gene knockdown of NHE1 and pNBC1 but not after control siRNA treatment. NHE1 inhibition has been shown to protect hippocampal neurons in a gerbil model of ischemic injury [43], where cell swelling was reduced as a result of decreased Na^+ entry caused by blockade of NHE1. The role of HCO_3^- transporters in the brain has been reported in a mouse model of prolonged hypoxia in which brain expression levels for two electro-neutral Na^+-coupled HCO_3^- transporters, (NBC3 and NDCBE) were decreased. This down-regulation of NBC3 and NDCBE in hypoxia resulted in cellular acidification

[44]. Thus, NHE1 and HCO_3^- transporters are critically important in maintaining ionic and pH homeostasis for neuronal survival.

In my experiments, I found that the neuronal excitability of TG neurons is affected by pH_i: intracellular alkalization increased AP firing rates, while acidification reduced them. The pH_i dependency of AP generation in TG neurons was further confirmed by altering the intracellular pH via the patch pipette in whole-cell mode. At pH_i 6.8, the AP firing rates mimicked the recordings in cell acidification, while at pH_i 7.8 the firing rates mimicked cell alkalization, equal to the early stage of the NH_4Cl pulse. These data are consistent with a previous report in hippocampal slices whereby ammonium prepulse induced bursting activity of CA3 neurons during the alkalinizations phase, and decreased spontaneous activities during the acidification phase [45].

The acidification induced by neurotransmitter receptor agonism promptly returned to baseline pH_i. Through a combination of pharmacological and siRNA knockdown approaches I demonstrate that the pH_i recovery mechanism in TG neurons is likely mediated by the membrane transporters NHE1 and pNBC1. Liu & Somps [46] have shown that inhibitors of NHE1 can reduce the excitability of rat primary sensory neurons. Together, my results extend these findings by demonstrating that the activity of plasma membrane Na^+/H^+ exchange, as well as Na^+/HCO_3^- co-transport, has consequences for sensory neuron excitability by directly affecting pH_i.

The regulation of pH_i is also critical for the behavior of other ion channel mechanisms. In rat hippocampal neurons, glutamate application induced cell acidification and reduced Ca^{2+} current amplitude, whereas intracellular alkalization potentiated Ca^{2+} current [47]. Also, acidification suppressed currents mediated by the murine TRPP3 channel, while alkalization caused an

increase in current amplitude [48]. pH_i has also been shown to modulate the capsaicin receptor TRPV1 itself, which may play a crucial role in the transmission of pain signals in DRG neurons [49].

In summary, Fig. 10 have been suggested mechanism that capsaicin-induced $[Ca^{2+}]_i$ increase causes intracellular acidification through the activity of PMCA3, and that the subsequent intracellular acidification is recovered by membrane transporters, including NHE1 and pNBC1 in TG neurons. I conclude that the activity of these transporters has direct consequences for sensory information flow through neuronal excitability regulation by pH_i change.

5. References

[1] R.S. Erzurumlu, Y. Murakami, F.M. Rijli, Mapping the face in the somatosensory brainstem, Nat Rev Neurosci 11 (2010) 252-263.

[2] M.C. Gonella, N.J. Fischbein, Y.T. So, Disorders of the trigeminal system, Semin Neurol 29 (2009) 36-44.

[3] J.M. Leston, [Functional anatomy of the trigeminal nerve], Neurochirurgie 55 (2009) 99-112.

[4] T.E. Taylor-Clark, M. Kollarik, D.W. MacGlashan, Jr., B.J. Undem, Nasal sensory nerve populations responding to histamine and capsaicin, J Allergy Clin Immunol 116 (2005) 1282-1288.

[5] M. Chesler, Regulation and modulation of pH in the brain, Physiol Rev 83 (2003) 1183-1221.

[6] A. Dhaka, V. Uzzell, A.E. Dubin, J. Mathur, M. Petrus, M. Bandell, A. Patapoutian, TRPV1 is activated by both acidic and basic pH, J Neurosci 29 (2009) 153-158.

[7] F. Fujita, K. Uchida, T. Moriyama, A. Shima, K. Shibasaki, H. Inada, T. Sokabe, M. Tominaga, Intracellular alkalization causes pain sensation through activation of TRPA1 in mice, J Clin Invest 118 (2008) 4049-4057.

[8] A.M. Vincent, M. TenBroeke, K. Maiese, Neuronal intracellular pH directly mediates nitric oxide-induced programmed cell death, J Neurobiol 40 (1999) 171-184.

[9] Y. Matsumoto, S. Yamamoto, Y. Suzuki, T. Tsuboi, S. Terakawa, N. Ohashi, K. Umemura, Na+/H+ exchanger inhibitor, SM-20220, is

protective against excitotoxicity in cultured cortical neurons, Stroke 35 (2004) 185-190.

[10] N. Hellwig, T.D. Plant, W. Janson, M. Schafer, G. Schultz, M. Schaefer, TRPV1 acts as proton channel to induce acidification in nociceptive neurons, J Biol Chem 279 (2004) 34553-34561.

[11] M.L. Wu, J.H. Chen, W.H. Chen, Y.J. Chen, K.C. Chu, Novel role of the Ca(2+)-ATPase in NMDA-induced intracellular acidification, Am J Physiol 277 (1999) C717-727.

[12] S.F. Pedersen, N.K. Jorgensen, I. Damgaard, A. Schousboe, E.K. Hoffmann, Mechanisms of pHi regulation studied in individual neurons cultured from mouse cerebral cortex, J Neurosci Res 51 (1998) 431-441.

[13] J.T. Daugirdas, J. Arrieta, M. Ye, G. Flores, D.C. Battle, Intracellular acidification associated with changes in free cytosolic calcium. Evidence for Ca2+/H+ exchange via a plasma membrane Ca(2+)-ATPase in vascular smooth muscle cells, J Clin Invest 95 (1995) 1480-1489.

[14] M.O. Bevensee, M. Apkon, W.F. Boron, Intracellular pH regulation in cultured astrocytes from rat hippocampus. II. Electrogenic Na/HCO3 cotransport, J Gen Physiol 110 (1997) 467-483.

[15] C. Vale-Gonzalez, A. Alfonso, C. Sunol, M.R. Vieytes, L.M. Botana, Role of the plasma membrane calcium adenosine triphosphatase on domoate-induced intracellular acidification in primary cultures of cerebelar granule cells, J Neurosci Res (2006).

[16] A. Gonzalez, P.J. Camello, J.A. Pariente, G.M. Salido, Free cytosolic calcium levels modify intracellular pH in rat pancreatic acini, Biochem Biophys Res Commun 230 (1997) 652-656.

[17] A. Gonzalez, J.A. Pariente, G.M. Salido, P.J. Camello, Intracellular pH and calcium signalling in rat pancreatic acinar cells, Pflugers Arch 434 (1997) 609-614.

[18] M.J. Caterina, M.A. Schumacher, M. Tominaga, T.A. Rosen, J.D. Levine, D. Julius, The capsaicin receptor: a heat-activated ion channel in the pain pathway, Nature 389 (1997) 816-824.

[19] L. Liu, S.A. Simon, Capsaicin, acid and heat-evoked currents in rat trigeminal ganglion neurons: relationship to functional VR1 receptors, Physiol Behav 69 (2000) 363-378.

[20] A. Patapoutian, A.M. Peier, G.M. Story, V. Viswanath, ThermoTRP channels and beyond: mechanisms of temperature sensation, Nat Rev Neurosci 4 (2003) 529-539.

[21] K.I. Takahashi, D.R. Copenhagen, Modulation of neuronal function by intracellular pH, Neurosci Res 24 (1996) 109-116.

[22] N. Abuladze, I. Lee, D. Newman, J. Hwang, K. Boorer, A. Pushkin, I. Kurtz, Molecular cloning, chromosomal localization, tissue distribution, and functional expression of the human pancreatic sodium bicarbonate cotransporter, J Biol Chem 273 (1998) 17689-17695.

[23] M.O. Bevensee, R.A. Weed, W.F. Boron, Intracellular pH regulation in cultured astrocytes from rat hippocampus. I. Role Of HCO3, J Gen Physiol 110 (1997) 453-465.

[24] Y.B. Kim, B.H. Yang, Z.G. Piao, S.B. Oh, J.S. Kim, K. Park, Expression of Na+/HCO3- cotransporter and its role in pH regulation in mouse parotid acinar cells, Biochem Biophys Res Commun 304 (2003) 593-598.

[25] K. Park, P.T. Hurley, E. Roussa, G.J. Cooper, C.P. Smith, F. Thevenod, M.C. Steward, R.M. Case, Expression of a sodium bicarbonate cotransporter in human parotid salivary glands, Arch Oral Biol 47 (2002) 1-9.

[26] S.P. Eckert, A. Taddese, E.W. McCleskey, Isolation and culture of rat sensory neurons having distinct sensory modalities, J Neurosci Methods 77 (1997) 183-190.

[27] G. Grynkiewicz, M. Poenie, R.Y. Tsien, A new generation of Ca2+ indicators with greatly improved fluorescence properties, J Biol Chem 260 (1985) 3440-3450.

[28] D. Lax, R. Martinez-Zaguilan, R.J. Gillies, Furazolidone increases thapsigargin-sensitive Ca(2+)-ATPase in chick cardiac myocytes, Am J Physiol 267 (1994) H734-741.

[29] T.D. Gover, T.H. Moreira, J.P. Kao, D. Weinreich, Calcium homeostasis in trigeminal ganglion cell bodies, Cell Calcium 41 (2007) 389-396.

[30] T. Brune, J.W. Deitmer, Intracellular acidification and Ca2+ transients in cultured rat cerebellar astrocytes evoked by glutamate agonists and noradrenaline, Glia 14 (1995) 153-161.

[31] C.K. Park, M.S. Kim, Z. Fang, H.Y. Li, S.J. Jung, S.Y. Choi, S.J. Lee, K. Park, J.S. Kim, S.B. Oh, Functional expression of thermo-transient receptor potential channels in dental primary afferent neurons: implication for tooth pain, J Biol Chem 281 (2006) 17304-17311.

[32] E.R. Partosoedarso, L.A. Blackshaw, Roles of central glutamate, acetylcholine and CGRP receptors in gastrointestinal afferent inputs to vagal preganglionic neurones, Auton Neurosci 83 (2000) 37-48.

[33] D.K. Lam, B.J. Sessle, J.W. Hu, Glutamate and capsaicin effects on trigeminal nociception I: Activation and peripheral sensitization of deep craniofacial nociceptive afferents, Brain Res 1251 (2009) 130-139.

[34] C. Vale-Gonzalez, A. Alfonso, C. Sunol, M.R. Vieytes, L.M. Botana, Role of the plasma membrane calcium adenosine triphosphatase on domoate-induced intracellular acidification in primary cultures of cerebelar granule cells, J Neurosci Res 84 (2006) 326-337.

[35] P. Kostyuk, E. Potapenko, I. Siryk, N. Voitenko, E. Kostyuk, Intracellular calcium homeostasis changes induced in rat spinal cord neurons by extracellular acidification, Neurochem Res 28 (2003) 1543-1547.

[36] C.J. Taylor, P.A. Nicola, S. Wang, M.A. Barrand, S.B. Hladky, Transporters involved in regulation of intracellular pH in primary cultured rat brain endothelial cells, J Physiol 576 (2006) 769-785.

[37] H.M. Prentice, Key contributions of the Na+/H+ exchanger subunit 1 and HCO3- transporters in regulating neuronal cell fate in prolonged hypoxia, Am J Physiol Regul Integr Comp Physiol 294 (2008) R448-450.

[38] J. Praetorius, Y.H. Kim, E.V. Bouzinova, S. Frische, A. Rojek, C. Aalkjaer, S. Nielsen, NBCn1 is a basolateral Na+-HCO3- cotransporter in rat kidney inner medullary collecting ducts, Am J Physiol Renal Physiol 286 (2004) F903-912.

[39] E. Roussa, W. Nastainczyk, F. Thevenod, Differential expression of electrogenic NBC1 (SLC4A4) variants in rat kidney and pancreas, Biochem Biophys Res Commun 314 (2004) 382-389.

[40] H. Yamada, S. Yamazaki, N. Moriyama, C. Hara, S. Horita, Y. Enomoto, A. Kudo, H. Kawakami, Y. Tanaka, T. Fujita, G. Seki, Localization of

NBC-1 variants in human kidney and renal cell carcinoma, Biochem Biophys Res Commun 310 (2003) 1213-1218.

[41] J. Li, N.Y. Koo, I.H. Cho, T.H. Kwon, S.Y. Choi, S.J. Lee, S.B. Oh, J.S. Kim, K. Park, Expression of the Na+-HCO3- cotransporter and its role in pHi regulation in guinea pig salivary glands, Am J Physiol Gastrointest Liver Physiol 291 (2006) G1031-1040.

[42] N.Y. Koo, J. Li, S.M. Hwang, S.Y. Choi, S.J. Lee, S.B. Oh, J.S. Kim, J.H. Lee, K. Park, Molecular cloning and functional expression of a sodium bicarbonate cotransporter from guinea-pig parotid glands, Biochem Biophys Res Commun 342 (2006) 1114-1122.

[43] J.W. Phillis, A.Y. Estevez, L.L. Guyot, M.H. O'Regan, 5-(N-Ethyl-N-isopropyl)-amiloride, an Na(+)-H(+) exchange inhibitor, protects gerbil hippocampal neurons from ischemic injury, Brain Res 839 (1999) 199-202.

[44] R.M. Douglas, J. Xue, J.Y. Chen, C.G. Haddad, S.L. Alper, G.G. Haddad, Chronic intermittent hypoxia decreases the expression of Na/H exchangers and HCO3-dependent transporters in mouse CNS, J Appl Physiol 95 (2003) 292-299.

[45] U. Bonnet, M. Wiemann, Ammonium prepulse: effects on intracellular pH and bioelectric activity of CA3-neurones in guinea pig hippocampal slices, Brain Res 840 (1999) 16-22.

[46] C.N. Liu, C.J. Somps, Na+/H+ exchanger-1 inhibitors reduce neuronal excitability and alter na+ channel inactivation properties in rat primary sensory neurons, Toxicol Sci 103 (2008) 346-353.

[47] L. Kiss, S.J. Korn, Modulation of N-type Ca2+ channels by intracellular pH in chick sensory neurons, J Neurophysiol 81 (1999) 1839-1847.

[48] T. Shimizu, A. Janssens, T. Voets, B. Nilius, Regulation of the murine TRPP3 channel by voltage, pH, and changes in cell volume, Pflugers Arch 457 (2009) 795-807.

[49] F. Fujita, K. Uchida, T. Moriyama, A. Shima, K. Shibasaki, H. Inada, T. Sokabe, M. Tominaga, Intracellular alkalization causes pain sensation through activation of TRPA1 in mice, J Clin Invest (2008).

국문 초록

삼차신경절 신경세포내 pH 조절기전에 관한 연구

황 성 민

서울대학교 대학원
치의과학과 신경생물학 전공
(지도교수: 박경표)

삼차신경절(Trigeminal ganglion)은 악안면 영역에서 치통을 포함한 다양한 구심성 신경 흥분을 전달하는 일차 감각성 뉴런이다. 삼차신경절에서는 다양한 신경전달 물질 및 효현제에 의해 세포내 칼슘 농도가 관찰된다. 하지만 이러한 세포내 칼슘의 농도 변화가 세포내 pH에 어떠한 영향을 미치는지, 그리고 변화된 세포내 pH가 자극이전의 수준으로 회복되는지에 대해서는 잘 알려져 있지 않다. 뿐 만 아니라 세포내 pH 회복 기전과 관련하여 어떤 종류의 세포막 수송체가 pH

회복에 관여하며, 그리고 이러한 세포내 pH의 변화가 삼차신경절 뉴런의 흥분성 조절에 어떠한 영향을 미치는지에 관해서는 알려진 바가 거의 없다. 본 연구는 삼차신경뉴런에서 세포내 칼슘 농도 변화와 세포내 pH의 연관성과 pH 회복에 관여하는 세포막 수송체 확인 및 활동전압에 미치는 영향을 규명하고자 하였다.

본 연구를 통해 삼차신경절내에서 transient receptor potential vanilloid 1 receptor 1 (TRPV1)의 활성을 통한 칼슘 증가는 plasma membrane Ca^{2+}/ATPase 3 (PMCA 3)의 활성을 통해 세포내 pH 감소를 유발한다는 것을 밝혀냈으며, 감소된 세포내 pH는 자극 이정의 수준으로 원상 회복되는데, 이 과정에서 세포막에 존재하는 pancreas type Na^+/HCO_3^- cotransporters 1 (pNBC1) 및 Na^+/H^+ exchangers 1 (NHE1)이 관여함을 확인하였다. 뿐만 아니라 세포내 pH 변화는 세포의 흥분성에도 크게 영향을 미쳐, 세포내 pH가 알칼리성일때는 활동 전압의 빈도가 증가한 반면 세포내 pH가 산성일때는 활동 전압의 빈도수가 감소함을 관찰하였다. 이러한 연구를 통해 세포내 pH의 변화는 활동 전압의 빈도에 많은 영향을 미친다는 것을 알 수 있다.

주요어: Trigeminal ganglion, PMCA3, pNBC1, NHE1

학 번: 2004-30761